PACS numbers: 07.79.Fc
DOI: 10.1070/QE2002v032n01ABEH002128

Superresolution at the singularities of phase images

A.V.Kretushev, V.P.Tychinskii

***Abstract*. Measurements performed with an Airyscan laser phase microscope showed the possibility of localisation of structural elements of a surface with a large gradient of the profile height and linear dimensions as small as 25 – 40 nm, which is 10 – 15 times lower than the Rayleigh criterion. The width of the structural elements was estimated from the extent of a region of the enhanced intensity of phase fluctuations. A metallised CD substrate with the known surface structure was used as a test object. Fluctuations of the optical path difference, whose intensity increased at steep profile slopes, were measured by periodically scanning the surface profile. It is shown that the extent of the region of enhanced intensity of phase fluctuations is close to the measured width of the steep profile slope. The intensity of fluctuations increased proportionally to the square of the height gradient, while their spatial extent decreased noticeably with increasing the objective aperture. These measurements explain a high sensitivity of the dynamic phase microscopy to fluctuations of the optical path difference in the regions of high gradient of the refractive index. The increase in the intensity at the slopes of the phase height profile and the spatial – temporal correlation of fluctuations were observed in mitochondria and other biological objects.**

Keywords: *optical path difference fluctuations, method of dynamic phase microscopy, intracellular dynamics, superresolution.*

1. Introduction

Points in the phase of interference images in the vicinity of which the amplitude of a signal tends to zero and its phase becomes ambiguous are called singularities. These singularities can appear in experiments in the regions of the object surface with a high steepness of the profile height and can be manifested as the wave-front dislocations or an increase in the intensity of phase fluctuations.

Recent interest in the living cell microscopy and the dynamics of macromolecules [1] stimulated the development and application of new optical methods featuring the high spatial and time resolution. Indeed, it seems that almost all intracellular processes are accompanied by local variations in the refractive index. For this reason, the interference methods, which are highly sensitive to variations in the optical path difference (OPD), proved to be useful for obtaining new information [2, 3].

The method of dynamic phase microscopy (DPM) [2, 3] allows the measurement of OPD fluctuations $h(x, y, t)$, which can be related in transparent media to the projection of the refractive index $n(x, y, z, t)$ on the image plane or to the movement of the object as a whole. The OPD fluctuations can be caused by the singularities and internal structure of the field, as well as by various external noises.

Several methods were proposed in paper [2] for analysing a change in the object state represented by its dynamic image $h(x, y, t)$. For example, track diagrams $h(x, t)$ could be obtained for the scan line chosen in the two-dimensional phase image of the object, which contained information required for calculating spatial – temporal correlation functions, spectral patterns, Fourier spectra, wavelets, etc.

Phase images have a number of unusual properties. For example, measurements of test objects with an Airyscan laser phase microscope [2 – 4] have demonstrated the possibility of increasing the spatial resolution by a factor of 3 – 5. The resolving power of a phase microscope depended not only on the numerical aperture A_n of the objective but also on the object structure, in particular, on the local OPD gradient. At singularities of phase images, the dislocations of the wave front can be also observed [7, 8], which are caused by the phase ambiguity in the vicinity of zeroes of the interference-field intensity. The profile slope dh/dx in this vicinity in the cross section of the phase image can be greater than the real 'geometrical' slope dH/dx. The characteristic feature of singularities is a large phase (or OPD) gradient dh/dx, which appears, as a rule, near a structural inhomogeneity of the object. In transparent media, singularities can be also caused by a large gradient of the refractive index.

The sensitivity to fluctuations of the object parameters and to the influence of external factors drastically increases in the vicinity of singularities. A similar increase in the intensity of fluctuations near the stability boundaries is well known in many fields of physics, for example, in the theory of oscillations and in the physics of phase transitions.

In the case of a surface with the submicron structure considered below, we assumed that the extent Δ of the region of high-intensity OPD fluctuations $I(x)$ is close to the width of δx of the profile part with a large height gradient. Because the values of $I(x)$ and Δ are averaged over a comparatively long time of measurements, the width Δ is

A.V.Kretushev, V.P.Tychinskii Moscow Institute of Radio Engineering, Electronics, and Automation, prosp. Vernadskogo 78, 117457 Moscow, Russia; e-mail: kretushev@mail.ru; vladimir@tych.pvt.msu.su

Received 14 June 2001
Kvantovaya Elektronika **32** (1) 66 – 70 (2002)
Translated by M.N.Sapozhnikov

statistically more reliable than one of the measurements of the profile width δx.

It is natural that the width Δ depends on the origin of the fluctuation source (it can be a characteristic of a particular microscope), the numerical aperture of the microscope objective, and the spatial resolution used in the measurement of dynamic processes. The corresponding resolution criterion for Δ, which can be adopted by one or another reasoning, can substantially differ from the Rayleigh criterion $R = 0.61\lambda/A_n$ [9, 10] established for a model of two identical incoherent point sources. For functional images, including phase images, there are no generally accepted resolution criteria. We will use in this paper the superresolution parameter in the form $S = R/\Delta \gg 1$, which takes into account both factors: the locality of the dynamic process and the numerical aperture of the objective.

The possibility of superresolution in the above sense is by no means obvious. The aim of the measurements presented below is to demonstrate the superresolution and to determine the conditions of its realisation in a model experiment with a surface with a submicron structure reflecting light. These results allow us to explain fluctuations in biological objects, where an increase in the intensity and the appearance of characteristic metabolic signals were observed in sites with the large OPD gradient [11, 12].

2. Results of measurements

The fabrication of an artificial object with a submicron dynamic profile is rather problematic, whereas natural biological objects (cells and organelles) are either unstable or some of their optical properties are unknown. For this reason, we used a structured metal CD substrate, assuming a priori that the more intense OPD fluctuations related to the intrinsic noise of a microscope will be observed at steep slopes of the surface profile.

The position of the scan line perpendicular to the tracks was fixed on the phase image of the substrate. Then, the track chart $h(x, t)$ was obtained by repeated scanning the profile $h(x)$ for 30 s and the intensity fluctuation distribution $I(x)$ was calculated. The measurements were performed with an Airyscan laser phase microscope [2–4] with $30^{\times}/0.65$, $50^{\times}/0.75$, and $100^{\times}/0.95$ objectives. The apparent profile slope dh/dx at the track boundary can be changed by rotating an object table. To detect steep parts of the profile $h(x)$, the focusing error should be no worse than 20 nm.

One can see from the track structure profile shown in Fig. 1a that the structure step was 1.6 μm, the width of the track was 800 nm, and the profile height was 120 nm. The change in the intensity $I(x)$ of fluctuations along the scan line is shown in Fig. 1b. The position of the intensity maxima coincided with the steep slopes of the profile, while their width Δ was close to the extent δx of the steep part of the slope. The width δx of steep slopes, the extent Δ of fluctuations, and the profile symmetry were measured by rotating the object table with a sample relative to the optical axis.

One of such asymmetric profiles measured using the $100^{\times}/0.95$ objective is shown in Fig. 2a. Figs 2b and 2c show the dependences of the intensity I and the slope dh/dx on x, which confirm the coincidence of their maxima. One can see that the widths of the maxima in this case were the same within the measurement error (±20 %) and equal to $\delta x \simeq \Delta = 25 \pm 5$ nm, which is substantially lower than the nominal resolution of the objective 400 nm. Similar results were obtained in measurements with other objectives. As the numerical aperture was decreased, the minimum width of the profile increased, while the intensity of fluctuations decreased. The results of measurements performed with the $50^{\times}/0.75$ objective are presented in Figs 2d–f.

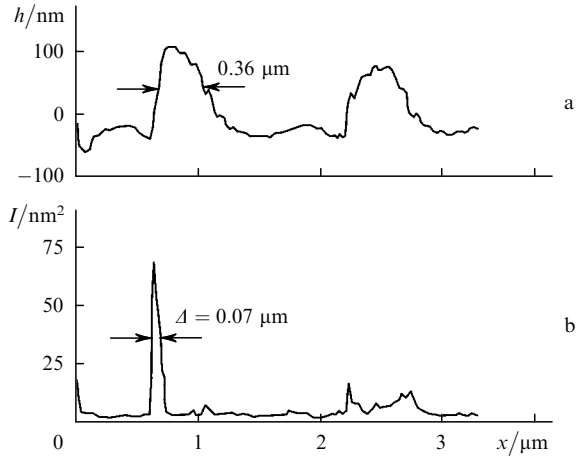

Figure 1. Profile $h(x)$ of a CD surface measured along a scan line, which demonstrates the characteristic structure of a track (a) and the intensity $I(x)$ of OPD fluctuations calculated from the track chart obtained upon the repeated scan of the profile $h(x, t)$ (b).

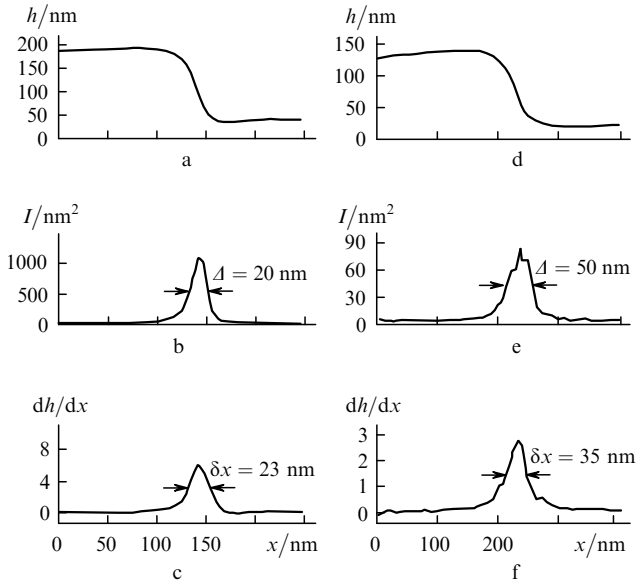

Figure 2. Asymmetric profiles $h(x)$ (a, d) and dependences of the OPD fluctuation intensity I (b, e) and the profile slope dh/dx (c, f) on x for measurements with the $100^{\times}/0.95$ (a–c) and $50^{\times}/0.75$ (d–f) objectives.

The approximately linear dependence $\delta x \simeq \Delta$ in a broad range of the slope variation follows from Figs 3 and 4. A large dispersion of the data is probably explained by the influence of various uncontrolled factors (acoustic noise, interferometer drift, etc.). The maximum intensity proved to be proportional to the square of the slope dh/dx: $I_{max} = C(dh/dx)^2$ (Fig. 4). Fig. 5 shows that the spectral density of fluctuations decreases monotonically with the frequency and the contrast components are absent.

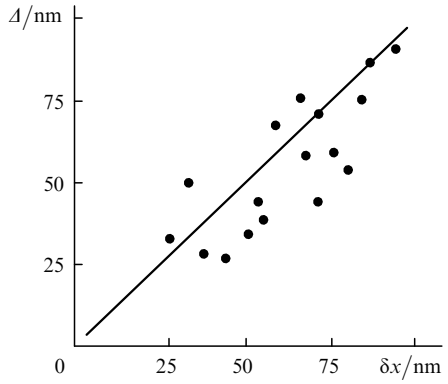

Figure 3. Dependence of the width Δ of regions of high-intensity OPD fluctuations on the width δx of the corresponding slopes with a large height gradient.

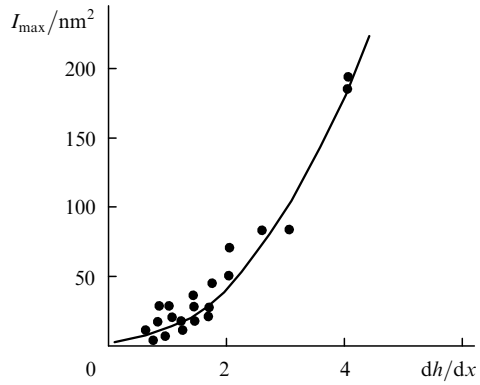

Figure 4. Dependence of the maximum intensity of OPD fluctuations for different parts of the profile on the corresponding slope dh/dx.

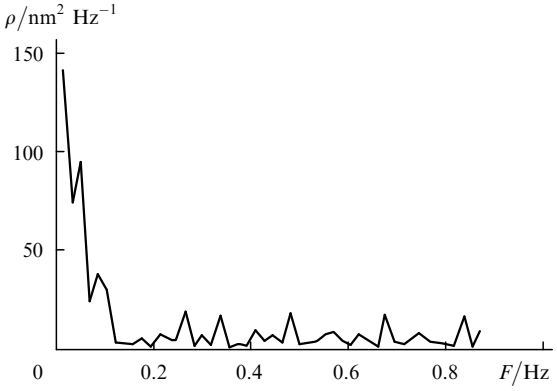

Figure 5. Dependence of the spectral density ρ of fluctuations on the frequency F (high-contrast components are absent).

3. Discussion and conclusions

The increase in the intensity of fluctuations at steep profile slopes can be simply explained, and the random nature of fluctuations is confirmed by a monotonic decrease of their spectral density with the frequency. The dependence $I(x)$ could be interpreted as the image of the time-averaged intensity distribution of fluctuations detected in the vicinity of a randomly moving surface element with the coordinate x_0 and the linear size δx.

However, in the case under study an object was immobile, and the lateral movement was simulated by the intrinsic noise of the instrument. We can estimate the root-mean-square amplitude δx_0 of fluctuations of lateral displacements taking into account the quadratic dependence of the intensity of OPD fluctuations on the profile slope: $I_{max} = C(\mathrm{d}h/\mathrm{d}x)^2$. For the dispersion $\langle(\delta x_0)^2\rangle = 30 - 40$ nm^2 (for $I_{max} \simeq 900$ nm^2 and $\mathrm{d}h/\mathrm{d}x \simeq 5.5$ from Figs 2b and 2c), we obtain the root-mean-square amplitude of the displacement of the point x_0 of the object $\delta x_0 \simeq 6$ nm and estimate the width of the distribution function as ~ 12 nm. The width $\Delta = 20$ nm measured directly proved to be close to this value.

Such an agreement was absent in the case of measurements with a $50^{\times}$ objective, which can be explained by a lower resolving power. The effect of the numerical aperture on the slope of the phase height is quite natural if we take into account the fact that the structure elements are smaller than the wavelength of light. However, a very strong dependence of the superresolution on the numerical aperture ($S = 1.5$ for $A_n = 0.65$, $S = 10$ for $A_n = 0.75$ and $S = 16$ for $A_n = 0.95$) proved to be unexpected. To explain this dependence, additional studies are required.

The results presented above illustrate the features of phase distortions and the possibilities of DPM, and show that the criterion of resolution of phase images should be refined.

The problem of superresolution has been studied in many papers, however, the resolution of functional images has not been adequately analysed. The measurements of submicron structured by phase methods involve inevitable systematic and random errors [6, 7] caused by high requirements to the focusing accuracy, the influence of polarisation and diffraction distortions, and by other technical factors. The correspondence between the phase images and a real object assumes knowledge of the optical parameters of the latter, so that the interpretation of the results of measurements is not always unambiguous.

Despite these limitations, the phase methods find wide applications in scientific instrument making due to their high sensitivity. One of the promising applications of phase microscopy, in particular DPM, is the measurement of intracellular dynamic processes.

In measurements of the surfaces of mitochondria and other organelles by the DPM method [2, 3, 11], an increase in the intensity of fluctuations was always observed at steep profiles of the phase height. In addition, high-contrast spectral components were present in the OPD fluctuation spectra. The linear size of the fluctuation region (50–100 nm) was sometimes close to the pixel size. When the size of isolated organelles was small, for example, in a suspension of mitochondria with diameter less than micrometer, along with endogenous biophysical processes related to the fermentative activity, the Brownian motion of organelles made a noticeable contribution to fluctuations.

In spectral patterns, low-frequency components corresponded to this motion, the extent of these components along a scan line being close to the mitochondrion diameter. The spectral density of fluctuations in these cases rapidly decreased with frequency. The endogenous processes related to the fermentative activity corresponded to less extended scan lines with contrast spectral components.

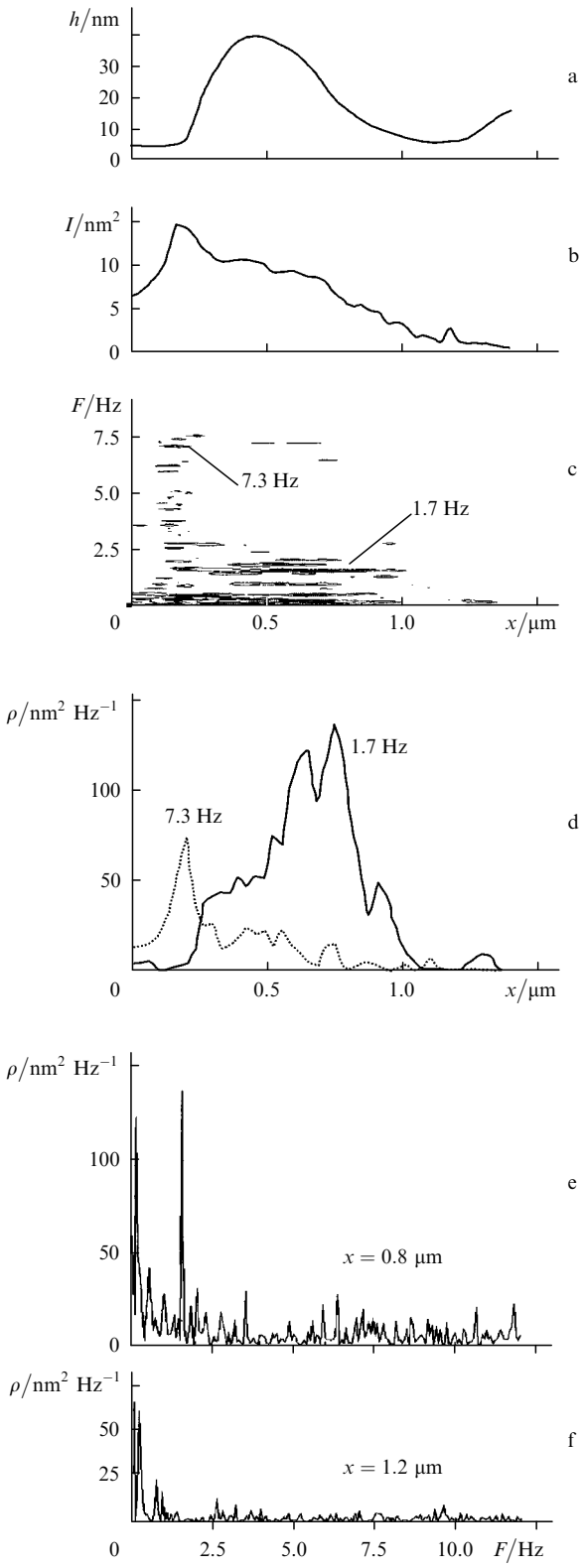

Figure 6. Measurements of OPD fluctuations in mitochondria: the phase height profile from which the mitochondrion diameter (~ 500 nm) and the slope ($dh/dx < 0.2$) were determined (a); the intensity of fluctuations in the vicinity of the steep slope of the height profile (b); the spectral portrait of fluctuations on the F, x plane which exhibits the extended low-frequency ($F < 1.2$ Hz) and comparatively short high-frequency components (c); the maxima of the spectral density ρ of components with $F = 1.7$ and 7.3 Hz located near steep slopes of the profile (d); and fluctuation spectra for $x = 0.8$ (e) and 1.2 μm (f).

In the general case, an immobile biological object in a buffer solution with the refractive index n_0 can be treated as an optical inhomogeneity $n(x, y, z, t)$ with the geometrical axial thickness $H(x, y, t)$. In a rather crude geometrical optics approximation, the phase image of the object can be represented in the form $dh/dx = H dn/dx + [(n - n_0) dH/dx]$. The OPD gradient $dh/dx = H dn/dx + (n - n_0) dH/dx$ in such a transparent medium depends both on variations in the refractive index $n(x, y, z, t)$ and on the geometrical thickness H. The intensity of fluctuations can increase at steep profile slopes and the spectral components with frequencies that are typical for $H(x, y, t)$ and $n(x, y, z, t)$ can appear. The separation of contributions from these two factors and the identification of signals are not trivial in the general case. However, when a priori information on the object structure is available, signals $h(x, y, t)$ can be interpreted quite reliably from the biophysical point of view.

As an example, we present in Fig. 6 the results of measurements of fluctuations in a mitochondrion [2, 11]. The phase height profile averaged for the measurement time of 30 s (Fig. 6a) does not reflect a complex internal structure of the mitochondrion. The mitochondrion diameter measured at the half-height was equal to 0.5 μm. The intensity distribution $I(x)$ of phase fluctuations in Fig. 6b is not smooth and has a maximum near the left steep part of the profile. One can see from the spectral pattern shown in Fig. 6c that the extension of low-frequency components ($F < 1.2$ Hz) is greater than the transverse size of the mitochondrion, while that of the higher-frequency is smaller.

The spectral density of components with frequencies 1.7 and 7.3 Hz is shown in Fig. 6d. The maxima of the component intensity are located near the steep slopes of the height profile. The spectral density changed noticeably at the segments of the scan line $\delta x_m = 50 - 80$ nm, which were substantially smaller than the slope width $\Delta x_m = 200$ nm. The fluctuation spectrum at the point $x = 0.8$ μm in Fig. 6e exhibits the high-contrast component with $F = 1.7$ Hz and the width of about 0.1 Hz. The extent of this component, which is comparable with the mitochondrion diameter, suggests that synchronous oscillations occurred at this frequency in a great part of the mitochondrion, which can be caused, for example, by regular variations in the membrane potential. The presence of more localised components can be explained by the activity of some groups of enzymes. Assuming that the total axial thickness of the mitochondrion membranes is $H \simeq 100$ nm, we can obtain from the intensity of the main component $I_{max} = 10$ nm^2 a rather realistic estimate of the change in the refractive index $\delta n = I_{max}^{1/2}/H = 0.03$.

Thus, an enhanced superresolution can be obtained at singularities of the phase images, and in particular, of dynamic specimens.

Acknowledgements. This work supported by the Innovations-Kolleg-27 grant of the University of Rostock (Germany).

References

1. Mehta A.D., Rief M., Spudich J.A., Smith D.A., Simmons R.M. *Science*, **283**, 1689 (1999).
2. Tychinskii V.P. *Usp. Fiz. Nauk*, **171**, 649 (2001).

3. Weiss D.G., Tychinsky V.P., Steffen W., Budde A. *Digital light microscopy techniques for the study of living cytoplasm in image analysis: methods and applications* (Boca Raton, CRC Press, 2000).
4. Tychinsky V., Masalov I., Pankov V., Ublinsky D. *Opt. Commun.*, **74**, 37 (1989).
5. Tychinskii V.P., Tavrov A.B., Shepel'skii D.V., Shchuchkin A.G. *Pis'ma Zh. Tekh. Fiz.*, **17**, 80 (1991).
6. Tychinskii V.P., Kufal' G.E., Vyshenskaya T.V., Perevedentseva E.V., Nikandrov S.L. *Kvantovaya Electron.* **24**, 754 (1997) [*Quantum Electron.*, **27**, 735 (1997)].
7. Tychinsky V.P. *Opt. Commun.*, **80**, 1 (1991).
8. Totzeck M., Tiziani H.J. *Opt. Commun.*, **138**, 365 (1997).
9. Solimeno S., Crosignani B., DiPorto P. *Guiding, diffraction, and confinement of optical radiation* (Orlando: Academic Press, 1986; Moscow: Mir, 1989).
10. Born M., Wolf E. *Principles of Optics, 4th ed.* (Oxford: Pergamon Press, 1969; Moscow: Nauka, 1970).
11. Tychinskii V.P., Weiss D., Vyshenskaya T.V., Yaguzhinskii L.S., Nikandrov S.L. *Biophys.*, **45**, 870 (2000).
12. Tychinsky V., Tavrov A., Shepelsky D., Vyshenskaja T. *Proc. SPIE Int. Opt. Soc. Eng.*, **1647**, 96 (1992).